Hyperfine Structure Constant of the Neutron Halo Nucleus $^{11}Be^+$

A. Takamine,[1,*] M. Wada,[1,†] K. Okada,[2] T. Sonoda,[1] P. Schury,[1] T. Nakamura,[3] Y. Kanai,[3] T. Kubo,[1] I. Katayama,[4] S. Ohtani,[5] H. Wollnik,[6] and H. A. Schuessler[7]

[1]*Nishina Center for Accelerator Based Science, RIKEN, 2-1 Hirosawa, Wako, Saitama 351-0198, Japan*
[2]*Department of Physics, Sophia University, 7-1 Kioicho, Chiyoda, Tokyo 102-8554, Japan*
[3]*Atomic Physics Laboratory, RIKEN, 2-1 Hirosawa, Wako, Saitama 351-0198, Japan*
[4]*Institute of Particle and Nuclear Studies, High Energy Accelerator Research Organization (KEK), Tsukuba, Ibaraki 305-0801, Japan*
[5]*Institute for Laser Science (ILS), The University of Electro-Communications, 1-5-1 Chofugaoka, Chofu, Tokyo 182-8585, Japan*
[6]*Department of Chemistry and Biochemistry, New Mexico State University, Las Cruces, New Mexico 88003, USA*
[7]*Department of Physics, Texas A&M University, College Station, Texas 77843, USA*

(Received 18 October 2012; revised manuscript received 15 January 2014; published 24 April 2014)

The hyperfine splittings of ground state $^{11}Be^+$ have been measured precisely by laser-microwave double resonance spectroscopy for trapped and laser cooled beryllium ions. The ions were produced at relativistic energies and subsequently slowed down and trapped at mK temperatures. The magnetic hyperfine structure constant of $^{11}Be^+$ was determined to be $A_{11} = -2677.302\,988(72)$ MHz from the measurements of the $m_F - m_F' = 0$–0 field independent transition. This measurement provides essential data for the study of the distribution of the halo neutron in the single neutron halo nucleus ^{11}Be through the Bohr-Weisskopf effect.

DOI: 10.1103/PhysRevLett.112.162502 PACS numbers: 21.10.Ky, 27.20.+n, 31.30.Gs, 37.10.Ty

The discovery of neutron halo nuclei in very neutron-rich unstable nuclei through interaction cross section measurements at intermediate energies [1] ignited various experimental and theoretical studies of such unstable nuclei. In recent years, high precision optical spectroscopy of halo nuclei has been performed and the charge radii of He, Li, and Be isotopes have been measured through isotope shifts [2–4]. We developed an online ion trap setup which converts radioactive nuclear ions from the GeV- to the μeV-energy scale and have measured the ground state hyperfine structure (hfs) splittings of all odd Be isotopes with high precision.

The magnetic hfs constant of the s state is a probe of the magnetization distribution of a nucleus which manifests itself under a local, *inhomogeneous* magnetic field due to the valence s electron, while the nuclear magnetic moment is an integrated magnetization measured with a *homogeneous* external field. A comparison of the ratio of the hfs constant A to the nuclear g factor among isotopes yields the Bohr-Weisskopf effect [5], which sensitively reflects the structure of the single neutron halo [6]. In a naive picture, the charge radius of ^{11}Be is representative of the core size while the magnetization radius represents the radius of the extended halo neutron since the nuclear magnetization of ^{11}Be is mainly carried by the halo neutron. Combined with the charge radii measurements [4,7], we can discern the neutron halo structure with the nuclear-model-independent optical probe.

The atomic states split into hyperfine levels identified by the quantum number $F = I + J$ where I and J are the nuclear and electronic spin quantum numbers, respectively. The magnitude of the splittings in the case of the magnetic dipole interaction is described as $H_{\rm hfs} = AIJ$ where A is the magnetic hyperfine constant. When an external magnetic field is applied, the hyperfine levels shift and split into magnetic sublevels due to the Zeeman effect. To determine the hfs constant A, the microwave transition frequency at zero magnetic field is the relevant quantity to measure. However, laser cooling is an essential prerequisite to resolve the hfs splittings of Be^+ ions, requiring a finite magnetic field for optical pumping into recyclable states. The pumping scheme is shown in Fig. 1 with the low-lying atomic levels of $^{11}Be^+$. With, for example, circularly polarized σ^+ laser radiation, the population is concentrated into the maximum m_F state and excitations and deexcitations are repeated between the states, $(2s^2S_{1/2}, F = 1, m_F = +1) \leftrightarrow (2p^2P_{3/2}, m_J = +3/2, m_I = +1/2)$. In this way, laser cooling is achieved and when additional microwave radiation resonant with ν^+ induces the transition between the hfs levels, the resonance can be detected as a decrease in the

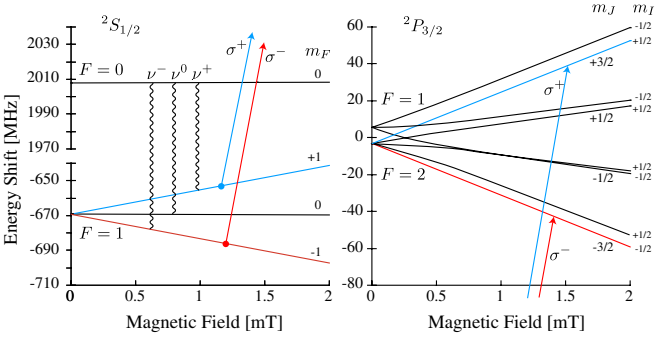

FIG. 1 (color online). Zeeman level diagram of the ground $2s^2S_{1/2}$ state and the excited $2p^2P_{3/2}$ state of $^{11}Be^+$. (Solid arrows are optical and curly lines represent microwave transitions.)

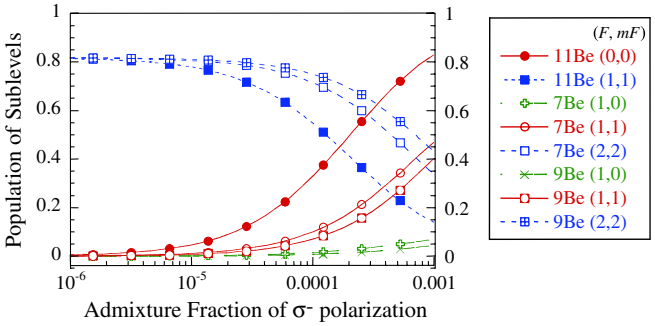

FIG. 2 (color online). Simulation results of optical pumping for $^{7,9,11}Be^+$ by incompletely polarized radiation under the condition that the magnetic field was 0.7 mT, the laser power 460 mW/cm^2, the ion temperature 0.2 K, the detuning frequency −40 MHz, and the dominant polarization of radiation σ^+. Ions were assumed to initially be equally distributed over all the m_F sublevels of the ground state.

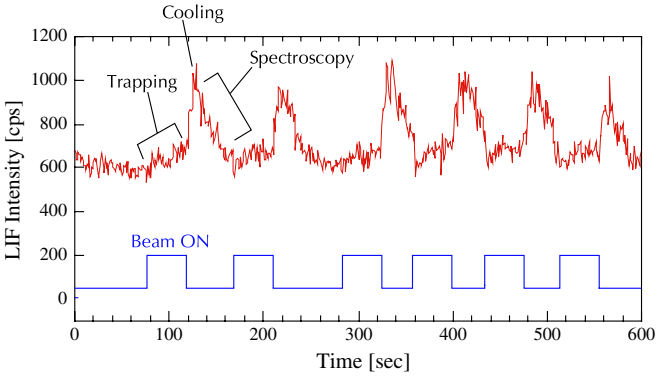

FIG. 3 (color online). Time sequence of the experiment. The cyclotron beam irradiated the target for 40 s and buffer gas was simultaneously applied to the trap during this period. After buffer gas was quickly evacuated, laser cooling occurs and spectroscopy was performed until the $^{11}Be^+$ ions had decayed.

fluorescence intensity. This is the scheme we have previously used for $^7Be^+$ [8]. However, the hfs transition frequency ν^+ is linearly dependent on the magnetic field with a relatively large coefficient of −14 MHz/mT which may cause serious line broadening due to the inhomogeneity of the applied magnetic field. An advantage of $^{11}Be^+$ over $^{7,9}Be^+$ is that the upper hfs level ($F = 0$) does not split because the nuclear spin is $I = 1/2$. If one can populate some fraction of atoms into the $F = 0$ state, one can measure the transition frequency between $(F, m_F) = (0, 0) \leftrightarrow (1, 0)$, which is field independent to first order.

We simulated the population of the ground state hfs levels of Be isotopes with incompletely polarized σ^+ radiation containing a small admixture of σ^- as shown in Fig. 2. A noticeable fraction of the population is seen in the $(F, m_F) = (0, 0)$ state only in $^{11}Be^+$ even with only a small admixture of counterpolarized radiation. Under such pumping conditions, resonance microwave radiation at ν_0 induces the $\Delta m_F = 0$ transition and the resonance can be detected as an increase in the fluorescence intensity. Figure 2 also shows that some fraction is in upper hfs levels of $^{7,9}Be^+$; however, they are dominantly in $(F, m_F) = (1, \pm 1)$ states and a very small fraction is seen in a $(F, m_F) = (1, 0)$ state. It is difficult to observe such a $m_F = m_F{}' = 0$ transition for $^{7,9}Be^+$ions.

The experiments were performed at the prototype SLOWRI facility at RIKEN. ^{11}Be ions were produced from the projectile fragmentation reaction induced by a ^{13}C beam at 100 A MeV on a 1850 mg/cm^2 ^9Be target. Many other nuclides were simultaneously produced and they were separated by the RIKEN projectile fragment separator RIPS [9]. After two wedged glass plates degraded their energy to less than 2 A MeV, the Be ions were thermalized in a gas catcher cell filled with 26 hPa of helium gas. They were guided by a rf carpet [10,11] to an exit nozzle, extracted from the gas cell, and transported to a high vacuum region through a 600 mm-long rf octupole ion beam guide (Carbon-OPIG) with differential pumping. A quadrupole mass filter removed most unwanted ions and the desired $^{11}Be^+$ ions were then trapped in a cryogenic linear rf trap using pulsed helium buffer gas cooling. In the trap, the temperature of Be^+ ions was further reduced by laser cooling using a UV laser resonant to the $2s^2S_{1/2} \rightarrow 2p^2P_{3/2}$ transition at 313 nm. In this experiment, 3×10^6 cps $^{11}Be^+$ ions were provided from the fragment separator and ions were extracted from the gas cell at about 70 cps. From the intensities of the laser-induced fluorescence (LIF) signal of $^{11}Be^+$ ions, we estimated that 110 ions were typically stored in the trap for each measurement. To directly measure the hfs transition frequencies of $^{11}Be^+$, we applied laser-microwave double resonance (LMDR) spectroscopy. The laser light and microwave were alternatively irradiated to avoid light shift and power broadening with a chopping rate of 4 kHz and a 60% duty for the laser. The microwave radiation was

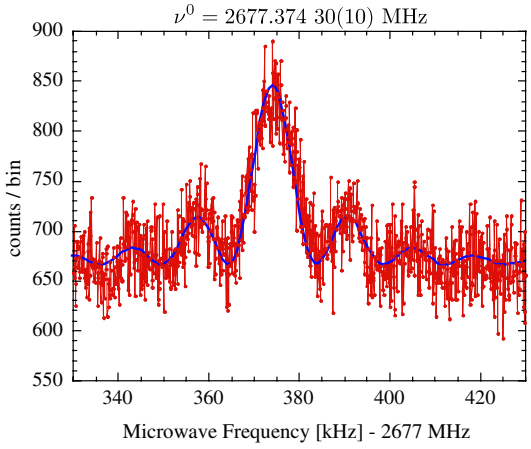

FIG. 4 (color online). Typical LMDR spectrum of the ground state hfs transition of $(F, m_F) = (0, 0) \rightarrow (1, 0)$ for $^{11}Be^+$ at a magnetic field $B = 0.698\,01(35)$ mT.

TABLE I. Resonance frequencies ν^0 for $^{11}Be^+$ at different magnetic field strengths.

I_{coil} [A]	B [mT]	ν^0 [MHz]
5	0.238 265(24)	2677.311 34(12)
14	0.698 01(35)	2677.374 30(10)
30	1.504 448(18)	2677.634 30(13)

generated by a synthesizer (HP8643A) whose clock was locked to a GPS frequency reference (Symmetricom 58503B). The LIF signal was detected by a two dimensional photon-counting system (PIAS-TI, Hamamatsu). This procedure is almost identical to the one used in the ^{7}Be experiment [8], with only the sequence of the measurement slightly different due to its shorter half-life of $T_{1/2} = 13.8$ s as shown in Fig. 3. $^{11}Be^+$ ions from the gas cell were accumulated for 40 s and immediately after evacuation of the buffer gas, the microwave frequency was scanned 10 times in 20 s before the $^{11}Be^+$ ions had decayed. Such a measurement cycle was repeated many times to achieve good statistics.

The field independent $m_F = m_F{}' = 0$ transition, $(F, m_F) = (0, 0) \rightarrow (1, 0)$, was measured at three different magnetic fields. Figure 4 is a typical LMDR spectrum indicating the fluorescence intensity as a function of the microwave frequency. The spectrum shows a Rabi resonance curve due to the pulsed microwave radiation. The resonance frequencies were obtained by least-square fitting to the transition probability function, $p(\Omega, b, \tau) = (2b^2/\Omega^2)(1 - \cos\Omega\tau)$, where b is the amplitude of the perturbation field, $\Omega = \sqrt{(\Delta\omega) + (2b^2)}$ the Rabi angular frequency, $\Delta\omega$ the detuning of microwave, and τ the duration of the perturbation field [12]. The resonance frequencies at three different magnetic fields are tabulated in Table I. The magnetic fields were determined from the hfs splittings of $^9Be^+$ ions under the same conditions. The error values for the magnetic fields stem from the statistics of spectra for $^9Be^+$. The electric current passing through the coils was stabilized using feedback measurements with a shunt resister that had a temperature coefficient of 5 ppm/K. The magnetic field drift between measurements of $^9Be^+$ and $^{11}Be^+$ thereby had a negligible effect on the frequency measurements. The $m_F = m_F{}' = 0$ transition still has a small quadratic dependence due to the magnetic field which is given by the Breit-Rabi formula. The transition frequency is described as

$$\nu^0(B) = \sqrt{A^2 + B^2 g_J^2 \mu_B^2 (1 - \gamma)^2}, \quad (1)$$

where A is the magnetic hfs constant, B the magnetic field strength, g_J the atomic g factor, μ_B the Bohr magneton, and γ the nuclear to atomic g-factor ratio. The resonance frequencies were fitted with this formula as shown in Fig. 5 and the transition frequency at the zero magnetic field was

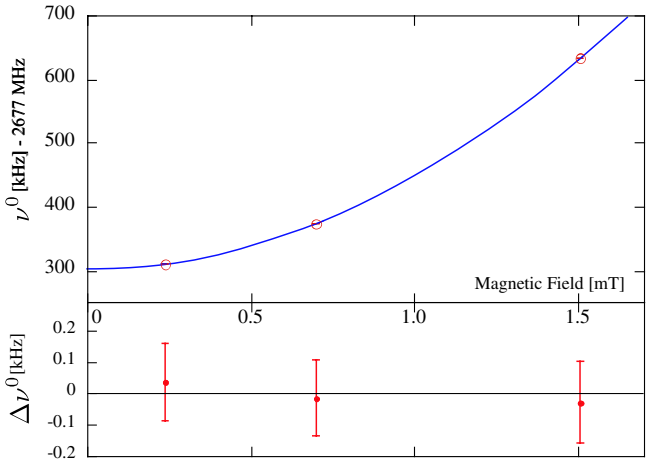

FIG. 5 (color online). Resonance frequencies ν^0 plotted as a function of the magnetic field fit to Eq. (1). The bottom indicates the difference between the experimental data and the fitting curve.

determined to be $\nu^0(0) = 2677.302\,988(72)$ MHz. The statistics and the error values for the magnetic fields contributed to this error value. There were no light shifts since the laser light was chopped by a blade and the precision of the microwave source is much higher than these measurements. Furthermore, we estimated the second-order Doppler shift and the quadratic Stark shift to be of orders 10^{-7} and 10^{-17} Hz, respectively, making them negligible.

The $\Delta m_F = \pm 1$ field dependent transitions, $(F, m_F) = (0, 0) \rightarrow (1, \pm 1)$, were also measured to confirm the sign of the hfs constant and the nuclear spin I. A typical spectrum is shown in Fig. 6 displaying a wider line width due to the inhomogeneity of the magnetic field. The resonance frequencies were obtained by fitting to the Rabi function and the results are compiled in Table II. The sign of the hfs constant of $^{11}Be^+$ is confirmed to be

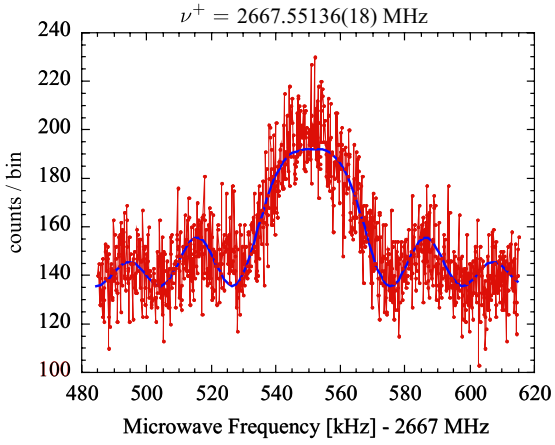

FIG. 6 (color online). Typical LMDR spectrum of the ground state hfs transition of $(F, m_F) = (0, 0) \rightarrow (1, +1)$ for $^{11}Be^+$ under the magnetic field $B = 0.696\,27(26)$ mT.

TABLE II. Resonance frequencies ν^+ and ν^- for $^{11}Be^+$ at different magnetic fields.

I_{coil} [A]	B [mT]	ν^+ [MHz]	ν^- [MHz]
12	0.596 01(14)	2668.9711(12)	
14	0.696 27(26)	2667.551 36(18)	2687.1260(44)
20	1.002 52(11)	2663.317 43(64)	2691.4385(42)
30	1.508 15(13)	2656.318 87(95)	

negative from $\nu^+ < \nu^-$. The dependence of the transition frequencies on the magnetic field is described as

$$\partial\nu^+/\partial B = -\mu_B 4I/(2I+1) \quad (2)$$

with $\mu_B = 14$ MHz/mT. The experimental result for ν^+ was -14 MHz/mT which is consistent with the nuclear spin $I = 1/2$. In total, the ground state hfs constant of $^{11}Be^+$ was determined to be $A_{11} = -2677.302\,988(72)$ MHz

The nuclear magnetic moment of ^{11}Be can be indirectly obtained from the hfs constant with a precision limited by the uncertainty of the hyperfine anomaly. The relation between the A/g ratio of two isotopes can be described as

$$A_{11}/g_{11} = A_9/g_9(1 + {}^{11}\Delta^9), \quad (3)$$

where $g = \mu_I/I$ is the nuclear g factor and $^{11}\Delta^9 \approx \epsilon_{BW}(^{11}\text{Be}) - \epsilon_{BW}(^{9}\text{Be})$ is the differential hyperfine anomaly which corresponds to the difference of the Bohr-Weisskopf effects (ϵ_{BW}) of the two isotopes. Diverse theoretical values for $^{11}\Delta^9$ were published based on different nuclear models. Fujita *et al.* [15] predicted $^{11}\Delta^9 = -4.68 \times 10^{-4}$ and -9.5×10^{-4} using a core plus neutron type wave function and a single-particle model with core polarization, respectively, while later on Parfenova and Leclercq-Willaim [16] calculated it, using a model that includes the halo effect, to be -3.2×10^{-4} and -1.9×10^{-4} for different weights of the s wave for the neutron. Taking the arithmetic average of the latter calculations, the nuclear magnetic moment of ^{11}Be can be evaluated to be $\mu_I(^{11}\text{Be}) = -1.68166(11)$ n.m., where the uncertainty reflects the possible variations within the model.

TABLE III. Magnetic hyperfine structure constants A of the ground $2s^2S_{1/2}$ state ions and nuclear magnetic moments for all odd beryllium isotopes.

Isotope	A [MHz]	μ_I [n.m.]	$(\mu_I$ [n.m.])[a]
^{7}Be	$-742.772\,28(43)$[c]		$-1.399\,28(2)$[c]
^{9}Be	$-625.008\,837\,048(10)$[d]	$-1.177\,432(3)$[e]	
^{11}Be	$-2677.302\,988(72)$[b]	$-1.6816(8)$[f]	$-1.681\,66(11)$[b]

[a]Indirectly from A.
[b]This work.
[c]Okada *et al.*, 2008 [8].
[d]Wineland *et al.*, 1983 [13].
[e]Itano, 1983 [14].
[f]Geithner *et al.*, 1999 [17].

In order to evaluate the magnetization distribution of the halo nucleus, the Bohr-Weisskpof effect should be experimentally determined. Table III summarizes presently known related data for all odd beryllium isotopes. Since there are no sufficiently precise measurements of the nuclear magnetic moments for the unstable beryllium isotopes, a direct measurement with the β-NMR method for ^{11}Be [17] can be temporarily used to evaluate the Bohr-Weisskopf effect to be $^{11}\Delta^9 = -2.2(4.7) \times 10^{-4}$. Obviously the limited precision of the $\mu_I(^{11}\text{Be})$ prohibits us to determine whether a finite hfs anomaly is present in the halo nucleus ^{11}Be. In a subsequent experiment, we will determine both the nuclear magnetic moment and the hyperfine constant simultaneously with high precision from the Zeeman splittings in a *strong* magnetic field as has been demonstrated for the stable ^{9}Be [18]. This method is also essential to determine μ_I of ^{7}Be, which does not emit β rays at all.

We acknowledge the crew of the RIKEN Nishina Center for Accelerator-based Science and Center for Nuclear Studies of University of Tokyo for their contribution to the online experiments. This work was supported by Grants-in-Aid for Scientific Research from the Japan Society for the Promotion Science, by the President's Special Grant of RIKEN, and by the Robert A. Welch Foundation under Grant No. A1546.

*Present address: Department of Physics and Mathematics, Aoyama Gakuin University, 5-10-1 Fuchinobe, Chuo, Sagamihara, Kanagawa 252-5258, Japan.
†mw@riken.jp

[1] I. Tanihata, T. Kobayashi, O. Yamakawa, S. Shimoura, K. Ekuni, K. Sugimoto, N. Takahashi, T. Shimoda, and H. Sato, Phys. Lett. B **206**, 592 (1988).
[2] P. Müller, I. A. Sulai, A. C. C. Villari, J. A. Alcántara-Núñez, R. Alves-Condé, K. Bailey, G. W. F. Drake, M. Dubois, C. Eléon, G. Gaubert, R. J. Holt, R. V. F. Janssens, N. Lecesne, Z.-T. Lu, T. P. O'Connor, M.-G. Saint-Laurent, J.-C. Thomas, and L.-B. Wang, Phys. Rev. Lett. **99**, 252501 (2007).
[3] R. Sánchez, W. Nörtershäuser, G. Ewald, D. Albers, J. Behr, P. Bricault, B. A. Bushaw, A. Dax, J. Dilling, M. Dombsky, G. W. F. Drake, S. Götte, R. Kirchner, H.-J. Kluge, Th. Kühl, J. Lassen, C. D. P. Levy, M. R. Pearson, E. J. Prime, V. Ryjkov, A. Wojtaszek, Z.-C. Yan, and C. Zimmermann, Phys. Rev. Lett. **96**, 033002 (2006).
[4] W. Nörtershäuser, D. Tiedemann, M. Žáková, Z. Andjelkovic, K. Blaum, M. L. Bissell, R. Cazan, G. W. F. Drake, C. Geppert, M. Kowalska, J. Kramer, A. Krieger, R. Neugart, R. Sánchez, F. Schmidt-Kaler, Z. C. Yan, D. T. Yordanov, and C. Zimmermann, Phys. Rev. Lett. **102**, 062503 (2009).
[5] A. Bohr and V. F. Weisskopf, Phys. Rev. **77**, 94 (1950).

[6] M. Wada, K. Okada, H. Wang, K. Enders, F. Kurth, T. Nakamura, S. Fujitaka, J. Tanaka, H. Kawakami, S. Ohtani, and I. Katayama, Nucl. Phys. **A626**, 365 (1997).
[7] A. Takamine, M. Wada, K. Okada, T. Nakamura, P. Schury, T. Sonoda, V. Lioubimov, H. Iimura, Y. Yamazaki, Y. Kanai, T. M. Kojima, A. Yoshida, T. Kubo, I. Katayama, S. Ohtani, H. Wollnik, and H. A. Schuessler, Eur. Phys. J. A **42**, 369 (2009).
[8] K. Okada, M. Wada, T. Nakamura, A. Takamine, V. Lioubimov, P. Schury, Y. Ishida, T. Sonoda, M. Ogawa, Y. Yamazaki, Y. Kanai, T. M. Kojima, A. Yoshida, T. Kubo, I. Katayama, S. Ohtani, H. Wollnik, and H. A. Schuessler, Phys. Rev. Lett. **101**, 212502 (2008).
[9] T. Kubo, M. Ishihara, N. Inabe, H. Kumagai, I. Tanihata, K. Yoshida, T. Nakamura, H. Okuno, S. Shimoura, and K. Asahi, Nucl. Instrum. Methods Phys. Res., Sect. B **70**, 309 (1992).
[10] M. Wada, Y. Ishida, T. Nakamura, Y. Yamazaki, T. Kambara, H. Ohyama, Y. Kanai, T. M. Kojima, Y. Nakai, N. Ohshima, A. Yoshida, T. Kubo, Y. Matsuo, Y. Fukuyama, K. Okada, T. Sonoda, S. Ohtani, K. Noda, H. Kawakami, and I. Katayama, Nucl. Instrum. Methods Phys. Res., Sect. B **204**, 570 (2003).
[11] A. Takamine, M. Wada, Y. Ishida, T. Nakamura, K. Okada, Y. Yamazaki, T. Kambara, Y. Kanai, T. M. Kojima, Y. Nakai, N. Oshima, A. Yoshida, T. Kubo, S. Ohtani, K. Noda, I. Katayama, P. Hostain, V. Varentsov, and H. Wollnik, Rev. Sci. Instrum. **76**, 103503 (2005).
[12] N. F. Ramsey, *Molecular Beams* (Oxford University Press, London, 1957), Chap. V.
[13] D. J. Wineland, W. M. Itano, and R. S. Van Dyck, Jr., Adv. At. Mol. Phys. **19**, 135 (1983).
[14] W. M. Itano, Phys. Rev. B **27**, 1906 (1983).
[15] T. Fujita, K. Ito, and T. Suzuki, Phys. Rev. C **59**, 210 (1999).
[16] Y. Parfenova and Ch. Leclercq-Willain, Phys. Rev. C **72**, 024312 (2005).
[17] W. Geithner, S. Kappertz, M. Keim, P. Lievens, R. Neugart, L. Vermeeren, S. Wilbert, V. N. Fedoseyev, U. Köster, V. I. Mishin, V. Sebastian, and ISOLDE Collaboration, Phys. Rev. Lett. **83**, 3792 (1999).
[18] T. Nakamura, M. Wada, K. Okada, I. Katayama, S. Ohtani, and H. A. Schuessler, Opt. Commun. **205**, 329 (2002).